

Extremum seeking control based on the super-twisting algorithm^{*}

Ixbalank Torres^{*} Fernando López-Caamal^{**}
Héctor Hernández-Escoto^{**} Alejandro Vargas^{***}

^{*} *C.A. Telemática, Departamento de Ingeniería Electrónica,
Universidad de Guanajuato, Carretera Salamanca-Valle de Santiago
Km. 3.5+1.8, Comunidad de Palo Blanco C.P. 36885, Salamanca,
Mexico. (e-mail: ixbalank@ugto.mx).*

^{**} *Departamento de Ingeniería Química, Universidad de Guanajuato,
Noria Alta C.P. 36050, Guanajuato, México (e-mail:
fernando.lopez@ugto.mx, hhee@me.com)*

^{***} *Laboratorio de Investigación en Procesos Avanzados de Tratamiento
de Aguas, Instituto de Ingeniería - UNAM, Av. Juriquilla 3001 C.P.
76230, Querétaro, Mexico (e-mail: avargasc@ingen.unam.mx)*

Abstract: This article addresses the problem of extremum seeking of a continuous-time dynamical system with a single input and a single output. First, a super-twisting-based gradient-based optimization algorithm is proposed to compute the input that leads to the extremum value of an unknown, convex objective function. Since the algorithm requires the input-output gradient of the system's response, a super-twisting based differentiator is proposed to compute the gradient using the measured output and the controlled input. Feasibility of the extremum seeking controller is demonstrated via closed-loop simulations over a microalgae production photobioreactor.

Keywords: Extremum seeking control, sliding modes, super-twisting algorithm, differentiators, process control.

1. INTRODUCTION

Extremum Seeking Control (ESC) is a model-free, real-time optimization tool applicable in situations where there is a nonlinearity in the optimization problem and such nonlinearity has a local minimum or maximum. The nonlinearity may be in the plant as a physical nonlinearity, possibly manifesting itself through an equilibrium map; or it may be in the control objective, via the cost functional of an optimization problem (Ariyur and Krstic, 2003).

Classical ESC aims to find an optimum input for a generally unknown objective function (or input-output map) and uses a dither signal to probe the input-output map so as to estimate an approximate gradient of this map (Tan et al., 2013).

In this century, due to their robustness properties against model uncertainties, sliding modes have been considered to propose robust ESC algorithms. For example, Yu and Ozguner (2003) propose an extremum-seeking control scheme enforced by a second order sliding mode control strategy. Angulo (2015) proposes an extremum seeking controller inspired in second order sliding modes to build an optimization framework for uncertain dynamic systems in which the variable to optimize is not measured and needs to be estimated. Lara-Cisneros et al. (2015) present an extremum-seeking control approach based on sliding

^{*} This work is supported by University of Guanajuato via the Institutional Project 358/2019.

modes to achieve the dynamic optimization of methane outflow rate in anaerobic digestion processes. In turn, Vargas et al. (2015) propose a feedback controller for fed-batch reactors that aims at regulating the substrate concentration at an optimum value, such that biomass production is enhanced while by-product formation is not favored. A virtual output is estimated using a bank of weighted super-twisting observers to drive an output-feedback extremum-seeking controller. Zeng et al. (2018) propose an extremum seeking control with the sliding mode method for a motor driving system with dead zone nonlinearity. Another interesting work is the article by Solis et al. (2019), in which, the authors present a continuous-time optimization method for an unknown convex function restricted to a dynamic plant with an available output including a stochastic noise. In order to reject the undesirable uncertainties and perturbations of the dynamic plant, the authors employ a standard deterministic integral sliding mode control.

In this paper, a super-twisting-based ESC algorithm is proposed to bypass the uncertainties in the input-output map. The proposed strategy consists of a gradient-based optimization algorithm coupled to a gradient estimator. In this light, the paper is organized as follows: in Section 2 the problem is formulated. In Section 3 the proposed super-twisting-based ESC algorithm is explained in detail, by introducing first the gradient-based optimizer and then the underpinning gradient estimator. In Section 4 the super-twisting-based ESC strategy is applied to a

microalgae production photobioreactor and the results are compared with the classical ESC. Finally, in Section 5 some conclusions regarding the proposed strategy are presented.

2. PROBLEM FORMULATION

Let us consider a dynamic system described by the following state space model

$$\begin{aligned} \dot{x}(t) &= f(x, u) \\ y(t) &= h(x, u) \end{aligned} \quad (1)$$

where $x \in \mathbb{R}^n$ is the state vector, $u \in \mathbb{R}$ is a controlled input and $y \in \mathbb{R}$ is the measured output.

In addition, let us consider an unknown function $y = l(u)$, with $l : U \subset \mathbb{R} \rightarrow \mathbb{R}$, an unimodal function which maps the input to the output in steady state, where U defines the operating region. Thus, the optimization problem to solve is stated as

$$\begin{aligned} \max_u l(u) \\ \text{such that:} \\ \dot{x}(t) &= f(x, u) \\ y(t) &= h(x, u) \end{aligned} \quad (2)$$

We adopt the following consideration:

Assumption 1. The function $l(u)$ is twice continuously differentiable with respect to u and has an unique maximizer u^* in an open neighborhood \mathcal{N} (Nocedal and Wright, 2000). Thus

$$\begin{aligned} \frac{\partial l}{\partial u}(u^*) &= 0, \\ \frac{\partial^2 l}{\partial u^2}(u^*) &< 0. \end{aligned}$$

The problem is then to propose an algorithm to find the optimum controlled input u^* in the neighborhood \mathcal{N} , such that the output y is maximized.

The optimization problem (2) can be solved by classical extremum-seeking control (ESC), which can be summarized as follows

$$\begin{aligned} u(t) &= \hat{u}(t) + A \sin(\omega t) \\ \dot{\hat{u}}(t) &= k_I \xi(t) \\ \xi(t) &= (y(t) - \eta(t)) A \sin(\omega t) \\ \dot{\eta}(t) &= -\omega_h \eta(t) + \omega_h y(t), \end{aligned} \quad (3)$$

where ξ is an approximation of the input-output map gradient, \hat{u} is the estimation of the optimum input, while A , ω , ω_h and k_I are design parameters.

In this work a super-twisting-based ESC algorithm is proposed to bypass the uncertainties in the input-output map. First, information about the controlled input and measured output is used to estimate the gradient $\partial y / \partial u$. Such a gradient estimation is then used by a gradient-based optimization algorithm to compute online the optimum controlled input.

3. SUPER-TWISTING BASED ESC

In this section the super-twisting based ESC proposed is developed in detail. We begin by presenting the gradient-

based optimization algorithm; then, the gradient estimation algorithm is described.

3.1 Gradient-based optimization

In order to compute the input u that maximizes the output $y = l(u)$, beginning at $u(0)$, gradient-based optimization algorithms generate a sequence of iterates $u(k)$, for $k = 0, 1, 2, \dots$, that terminate when either no more progress can be made or when it seems that a solution value has been approximated with sufficient accuracy. In deciding how to move from one iterate $u(k)$ to the next, the algorithm avails of the gradient $\partial l / \partial u$. It is the direction along which the objective function $l(u)$ grows most rapidly. In general, gradient-based optimization algorithms use this information to find a new iterate $u(k+1)$ which yields a larger value of y than the one produced by $u(k)$ (Nocedal and Wright, 2000).

Thus, the new iterate $u(k+1)$ can be computed as

$$u(k+1) = u(k) + \alpha_d \frac{\partial l}{\partial u}; \alpha_d > 0, \quad (4)$$

where α_d is the distance to move along the gradient.

Let us define $\alpha_d := \alpha \Delta t$, with $\Delta t := t(k+1) - t(k)$. By replacing it in (4) we have

$$u(k+1) = u(k) + \alpha \Delta t \frac{\partial l}{\partial u}$$

or

$$\frac{\Delta u}{\Delta t} = \alpha \frac{\partial l}{\partial u}.$$

By applying the limit when $\Delta t \rightarrow 0$, the gradient-based extremum-seeking algorithm is obtained

$$\dot{u}(t) = \alpha \frac{\partial l}{\partial u}; \alpha > 0. \quad (5)$$

Let $e(t) := l(u^*) - l(u(t))$, which represents the difference between the maximum output and the output at a time t . Now, let us consider the following Lyapunov function candidate

$$V(e) = e(t). \quad (6)$$

Since $l(u^*) \geq l(u(t))$ for any t , $V(e)$ is positive definite. On the other hand, $\dot{V}(e)$ is given by

$$\dot{V}(e) = \dot{e}(t) = -\frac{\partial l}{\partial u} \dot{u}(t) = -\alpha \left(\frac{\partial l}{\partial u} \right)^2 \leq 0.$$

Thus, the asymptotic stability of the error dynamics is assured and therefore the output $y(u(t))$ asymptotically approaches the maximum output $y(u^*)$ (Zhang and Ordonez, 2012).

Since the optimization algorithm (5) uses the gradient $\partial l / \partial u$ but $l(u)$ is an unknown function, in real applications either an approximation or an estimation of such a gradient must be considered.

In order to bypass the uncertainty related to the unknown function $l(u)$, let us consider not the gradient but the sign of the gradient in the algorithm (5), which, indeed, contains the direction information. A robust optimization algorithm can then be proposed as

$$\dot{u}(t) = \alpha \operatorname{sign} \left(\frac{\partial l}{\partial u} \right); \alpha > 0. \quad (7)$$

with the sign function defined as

$$\text{sign}(\sigma) = \begin{cases} 1; & x > 0 \\ -1; & x < 0 \end{cases}$$

and $\text{sign}(0) \in [-1, 1]$ (Shtessel et al., 2014).

Taking into account the positive definite candidate Lyapunov function (6), the derivative $\dot{V}(e)$ is given by

$$\begin{aligned} \dot{V}(e) &= \dot{e}(t) = -\frac{\partial l}{\partial u} \dot{u}(t) = -\alpha \frac{\partial l}{\partial u} \text{sign} \left(\frac{\partial l}{\partial u} \right) \\ \dot{V}(e) &= -\alpha \left| \frac{\partial l}{\partial u} \right| \leq 0. \end{aligned}$$

Again, the asymptotic stability of the error dynamics is assured and therefore the output $y(u(t))$ asymptotically approaches the maximum output $y(u^*)$ (Zhang and Ordonez, 2012).

Equation (7) induces a first order sliding mode, with the gradient $\sigma = \partial l / \partial u$ as the sliding variable. Furthermore, it has the form of the integral part of the super-twisting algorithm with sliding variable defined as $\sigma = -\partial l / \partial u$. By accounting for these observations, the following theorem describes our strategy, which avails of a second order sliding mode.

Theorem 1. Let us consider the super-twisting algorithm

$$\begin{aligned} u(t) &= -\lambda |\sigma|^{1/2} \text{sign}(\sigma) + u_1(t), \\ \dot{u}_1(t) &= -\alpha \text{sign}(\sigma), \end{aligned} \quad (8)$$

where $\lambda > 0$ and $\alpha > 0$ are constant gains and σ is a sliding variable (Shtessel et al., 2014).

By considering $\sigma = -\partial l / \partial u$, the algorithm (8) asymptotically maximize the objective function $l(u)$.

Proof. By taking into account the positive definite candidate Lyapunov function (6), the derivative $\dot{V}(e)$ is given by

$$\dot{V}(e) = \dot{e}(t) = -\frac{\partial l}{\partial u} \dot{u}(t),$$

where $\dot{u}(t)$ is given by

$$\begin{aligned} \dot{u}(t) &= \lambda \text{sign} \left(\frac{\partial l}{\partial u} \right) \left[\frac{1}{2} \left| \frac{\partial l}{\partial u} \right|^{-1/2} \frac{d}{dt} \left| \frac{\partial l}{\partial u} \right| \right] + \dot{u}_1(t) \\ \dot{u}(t) &= \lambda \text{sign} \left(\frac{\partial l}{\partial u} \right) \left[\frac{1}{2} \left| \frac{\partial l}{\partial u} \right|^{-1/2} \text{sign} \left(\frac{\partial l}{\partial u} \right) \frac{\partial^2 l}{\partial u^2} \dot{u}(t) \right] \\ &\quad + \alpha \text{sign} \left(\frac{\partial l}{\partial u} \right) \\ \dot{u}(t) &= \frac{\lambda}{2 \left| \frac{\partial l}{\partial u} \right|^{1/2}} \frac{\partial^2 l}{\partial u^2} \dot{u}(t) + \alpha \text{sign} \left(\frac{\partial l}{\partial u} \right) \\ \dot{u}(t) &= \frac{\alpha}{1 - \frac{\lambda}{2 \left| \frac{\partial l}{\partial u} \right|^{1/2}} \frac{\partial^2 l}{\partial u^2}} \text{sign} \left(\frac{\partial l}{\partial u} \right). \end{aligned}$$

According to the Taylor's theorem, the function $l(u)$ can be approximated as

$$\begin{aligned} l(u^* + h) &= l(u^*) + h \frac{\partial l}{\partial u}(u^*) + \frac{h^2}{2} \frac{\partial^2 l}{\partial u^2}(u^*) + \dots \\ &\quad + \frac{h^{n-1}}{(n-1)!} \frac{\partial^{n-1} l}{\partial u^{n-1}}(u^*) + \frac{h^n}{n!} \frac{\partial^n l}{\partial u^n}(u^* + \theta h) \end{aligned}$$

for $\theta \in (0, 1)$.

If $n = 2$, due to Assumption 1,

$$l(u^* + h) - l(u^*) = \frac{h^2}{2} \frac{\partial^2 l}{\partial u^2}(u^* + \theta h) < 0,$$

and therefore

$$\frac{\partial l^2}{\partial u^2}(u) < 0$$

in a neighborhood \mathcal{N} of u^* .

Hence

$$\dot{u}(t) = \alpha' \text{sign} \left(\frac{\partial l}{\partial u} \right),$$

where

$$\alpha' = \frac{\alpha}{1 - \frac{\lambda}{2 \left| \frac{\partial l}{\partial u} \right|^{1/2}} \frac{\partial^2 l}{\partial u^2}} > 0.$$

Thus

$$\dot{V}(e) = -\alpha' \frac{\partial l}{\partial u} \text{sign} \left(\frac{\partial l}{\partial u} \right) = -\alpha' \left| \frac{\partial l}{\partial u} \right| \leq 0.$$

The asymptotic stability of $e(t)$ is then assured and therefore, the output $y(u(t))$ asymptotically approaches the maximum output $y(u^*)$. \square

Please notice that the framework of this theorem is exactly the same as for the ESC, in the sense that is a model-free approach applicable to a convex steady-state map. Thus, when such control law is applied to the plant, the sliding variable converges to the origin; that is $\sigma \rightarrow 0$. In light of Assumption 1, this implies the convergence to the extreme value of $l(u)$.

Remark 1. Note that the super-twisting algorithm includes a proportional action and an integral action. By considering the sign of the gradient in both terms, the robustness of the optimization algorithm is enhanced. On the other hand, the term $|\partial l / \partial u|^{1/2}$ in the proportional term acts as an adaptive gain. Since the initial condition $u(0)$ is in a neighborhood of u^* , normally $|\partial l / \partial u| < 1$. Hence, the term $\lambda |\partial l / \partial u|^{1/2}$ assures that $u(t)$ will approach to u^* faster than $u_1(t)$.

Remark 2. Minimization problems can be solved by using the gradient-based optimization algorithm (8). In such a case, the sliding variable $\sigma = \partial l / \partial u$ must be considered. The convergence proof is similar to the proof previously presented.

In the following section, we provide an estimation of the input-output gradient, via a signals differentiator based on the super-twisting algorithm.

3.2 Gradient Estimation

In order to obtain an online input-output gradient estimation, $\partial y / \partial u$, we consider the parametric differentiation. That is

$$\frac{\partial y}{\partial u} = \frac{dy/dt}{du/dt}, \quad (9)$$

provided the time-derivatives of $y(t)$ and $u(t)$ exist and $du(t)/dt \neq 0$.

Thus, for achieving an estimation of the gradient, we may first obtain an online estimation of $y(t)$'s and $u(t)$'s derivative.

To this end, let us define

$$\boldsymbol{\theta} := \begin{pmatrix} y \\ u \end{pmatrix}, \quad (10)$$

with first time-derivative.

$$\boldsymbol{\omega} := \begin{pmatrix} \dot{y} \\ \dot{u} \end{pmatrix}, \quad (11)$$

The following theorem presents a system capable of estimating $\boldsymbol{\omega}$, which is adapted from (López-Caamal and Moreno, 2019).

Theorem 2. Let

$$\begin{aligned} \dot{\hat{\boldsymbol{\theta}}}(t) &= -k_1 \boldsymbol{\phi}^1(\hat{\boldsymbol{\theta}} - \boldsymbol{\theta}) + \hat{\boldsymbol{\omega}}(t) \\ \dot{\hat{\boldsymbol{\omega}}}(t) &= -k_2 \boldsymbol{\phi}^2(\hat{\boldsymbol{\theta}} - \boldsymbol{\theta}), \end{aligned} \quad (12)$$

where $\hat{\boldsymbol{\theta}}$ ($\hat{\boldsymbol{\omega}}$, resp.) denote the estimation of $\boldsymbol{\theta}$ ($\boldsymbol{\omega}$, resp.). Furthermore, let us assume that $\hat{\boldsymbol{\omega}}$ is element-wise bounded; and let the functions $\boldsymbol{\phi}^i(\mathbf{x})$ be

$$\begin{aligned} \boldsymbol{\phi}^1(\mathbf{x}) &= \left(\eta \|\mathbf{x}\|_2^{-p} + \beta + \gamma \|\mathbf{x}\|_2^q \right) \mathbf{x}, \quad \boldsymbol{\phi}^1(\mathbf{0}) := \mathbf{0}, \\ \boldsymbol{\phi}^2(\mathbf{x}) &= \left(\eta(1-p) \|\mathbf{x}\|_2^{-p} + \beta + \gamma(1+q) \|\mathbf{x}\|_2^q \right) \boldsymbol{\phi}^1(\mathbf{x}). \end{aligned} \quad (13)$$

If the constants $\eta, \beta, \gamma > 0$, $\frac{1}{2} \geq p > 0$, and $q > 0$; and k_1 and k_2 are chosen such that the matrix

$$\mathbf{A} = \begin{pmatrix} -k_1 & 1 \\ -k_2 & 0 \end{pmatrix} \quad (14)$$

is Hurwitz, the origin of the estimation error is finite-time stable.

Proof. By letting $\mathbf{x} := \hat{\boldsymbol{\theta}} - \boldsymbol{\theta}$ and $\mathbf{z} := \hat{\boldsymbol{\omega}} - \boldsymbol{\omega}$, the differentiation error becomes

$$\begin{aligned} \dot{\mathbf{x}}(t) &= -k_1 \boldsymbol{\phi}^1(\mathbf{x}) + \mathbf{z}(t) \\ \dot{\mathbf{z}}(t) &= -k_2 \boldsymbol{\phi}^2(\mathbf{x}) - \mathbf{z}(t). \end{aligned}$$

In turn, the origin of differentiation error is finite-time stable as studied via the following Lyapunov function

$$V = \begin{pmatrix} \boldsymbol{\phi}^1(\mathbf{x}) \\ \mathbf{z} \end{pmatrix}^\top [\mathbf{P} \otimes \mathbf{I}] \begin{pmatrix} \boldsymbol{\phi}^1(\mathbf{x}) \\ \mathbf{z} \end{pmatrix},$$

whose time-derivative is

$$\dot{V} = - \begin{pmatrix} \boldsymbol{\phi}^1(\mathbf{x}) \\ \mathbf{z} \end{pmatrix}^\top [\mathbf{Q} \otimes \mathbf{J}(\mathbf{x})] \begin{pmatrix} \boldsymbol{\phi}^1(\mathbf{x}) \\ \mathbf{z} \end{pmatrix}.$$

Here the matrices $\mathbf{P}, \mathbf{Q} \in \mathbb{R}^{2 \times 2}$ satisfy the Algebraic Lyapunov Equation $\mathbf{P}\mathbf{A} + \mathbf{A}^\top \mathbf{P} = -\mathbf{Q}$; given that \mathbf{A} is Hurwitz and by choosing a $\mathbf{Q} = \mathbf{Q}^\top > 0$, then \mathbf{P} is symmetric and positive definite. In turn, the matrix

$$\begin{aligned} \mathbf{J}(\mathbf{x}) &:= \nabla_{\mathbf{x}} \boldsymbol{\phi}^1(\mathbf{x}) \\ &= \left(\eta \|\mathbf{x}\|_2^{-p} + \beta + \gamma \|\mathbf{x}\|_2^q \right) \mathbf{I}_n \\ &\quad + \left(\gamma q \|\mathbf{x}\|_2^q - \eta p \|\mathbf{x}\|_2^{-p} \right) \frac{\mathbf{x}\mathbf{x}^\top}{\mathbf{x}^\top \mathbf{x}} \end{aligned}$$

is symmetric and positive definite. Additionally \otimes denotes the Kronecker product. Please notice that for square matrices \mathbf{A}, \mathbf{B} with eigenvalues λ_i and ν_j , the eigenvalues of $\mathbf{A} \otimes \mathbf{B}$ are $\lambda_i \nu_j \forall i, j$. Hence, both $\mathbf{P} \otimes \mathbf{I}$ and $\mathbf{Q} \otimes \mathbf{J}(\mathbf{x})$ are

symmetric and positive definite matrices, which shows the asymptotic stability of the origin. The proof of finite-time stability may be found in (López-Caamal and Moreno, 2019, §4.2). \square

Please notice that the previous differentiator provides an estimate of the first time-derivative of $y(t)$ and $u(t)$, which may be used to estimate the input-output gradient, as described in (9). Both estimates converge exactly at the same time due to the nonlinearity $\boldsymbol{\phi}^1(\mathbf{x})$, which couple the differentiator's states and becomes zero only when $\mathbf{x} = \mathbf{0}$. In addition to the convergence timing, another advantage of using a multivariable differentiator is that we only need to design one algorithm for both differentiation tasks. For further robustness properties of (12), we refer the interested reader to (López-Caamal and Moreno, 2019). The following section demonstrate applicability of our ESC via numerical simulations.

4. RESULTS

Let us consider a microalgae production process developed by Benavides et al. (2015). In this process, the growth of microalgae under substrate limitation is represented by the Droop model, which is given by the following ODE system

$$\begin{aligned} \dot{S}(t) &= -\rho(S)X(t) + \frac{Q_{in}(t)}{V} (S_{in}(t) - S(t)) \\ \dot{Q}(t) &= \rho(S) - \mu(Q)Q(t) \\ \dot{X}(t) &= \mu(Q)X(t) - \frac{Q_{in}(t)}{V} X(t). \end{aligned} \quad (15)$$

Here S in ($g L^{-1}$) is the substrate concentration in the culture medium; Q in ($g g^{-1}$) is the internal carbon-based quota of substrate; X in ($g L^{-1}$) is the biomass concentration in the culture medium; S_{in} in ($g L^{-1}$) is the substrate concentration in the renewal medium; Q_{in} in ($L d^{-1}$) is the flow rate in the renewal medium; and V in (L) is the volume of the culture. The functions ρ and μ represent substrate uptake and growth rate, respectively. In this model the specific uptake ρ and growth rate μ are Michaelis-Menten and Droop functions, respectively:

$$\rho(S) = \rho_{max} \frac{S}{K_S + S}, \quad (16)$$

where ρ_{max} is the maximum limiting substrate uptake rate and K_S is the half saturation constant of substrate; and,

$$\mu(Q) = \mu_{max} \left(1 - \frac{Q_0}{Q} \right), \quad (17)$$

where μ_{max} is the maximum growth rate and Q_0 is the minimum cell quota identified empirically by Droop under which microalgae do no longer grow (Benavides et al., 2015).

We are interested in maximizing the productivity of the microalgae production process in real-time. Such an optimization problem can be stated as

$$\begin{aligned} &\max_{Q_{in}} P(Q_{in}) \\ &\text{such that:} \\ &\dot{x}(t) = f(x, Q_{in}) \\ &y(t) = P(x, Q_{in}), \end{aligned} \quad (18)$$

Table 1. Table of parameters

Classical ESC	Fast ST-ESC	Slow ST-ESC
$\omega = 0.175$	$\alpha = 0.1$	$\alpha = 0.01$
$\omega_h = 0.9\omega$	$\lambda = 0.5$	$\lambda = 0.05$
$A = 0.25$	$\eta = 50$	$\eta = 50$
$k_I = 2$	$\beta = 5$	$\beta = 5$
	$\gamma = 15$	$\gamma = 15$
	$p = 0.25$	$p = 0.25$
	$q = 5$	$q = 5$
	$k_1 = 1$	$k_1 = 1$
	$k_2 = 1$	$k_2 = 1$

where $x = [SQX]^\top$, $f(x, Q_{in})$ is defined according to Equation (15) and the measured output $P(x, Q_{in})$ is the productivity of the process, defined as

$$P(x, Q_{in}) = \frac{Q_{in}(t)X(t)}{V}. \quad (19)$$

A similar optimization problem has been addressed by considering classical ESC (Dewasme et al., 2017). As mentioned by Dewasme et al. (2017), achieving the optimum by the extremum-seeking strategies (5) and (8)-(12) is only possible if it corresponds to an equilibrium of the model (15). Hence, the equilibria of the open-loop photobioreactor should be first determined. This equilibria for the model (15) have to be, therefore, calculated. By equating the right-hand side of (15) to zero, and solving the resulting nonlinear algebraic equations, the following objective function in steady state is obtained:

$$P(Q_{in}) = \frac{a_3 Q_{in}^3 + a_2 Q_{in}^2 + a_1 Q_{in}}{a_4 Q_{in} + a_5}, \quad (20)$$

where a_1, a_2, a_3, a_4 , and a_5 are constants. The optimum value Q_{in}^* is obtained by differentiating (20) with respect to Q_{in} and equating the result to zero (first-order optimality condition in Assumption 1), which leads to $Q_{in}^* = 11.46 Ld^{-1}$. By substituting Q_{in}^* in (20), a maximum productivity $P_{max} = 6.08 gL^{-1}d^{-1}$ is obtained.

Simulations of the ESC (5) and the super-twisting-based ESC (8)-(12) were performed in Matlab. The model (15) and the ODEs involved in the ESC (5) and (8)-(12) were solved using the stiff solver *ode15s*. A constant substrate concentration at the photobioreactor input $S_{in} = 0.5 gL^{-1}$ was considered. The online optimization started fifty days after the bioprocess simulation beginning. An optimization period $\Delta t = 2d$ was considered for the ESC strategy (5), while an optimization period $\Delta t = 5d$ was considered for the super-twisting-based ESC (8)-(12). Additionally, we consider that the signals to differentiate are $\theta = [P Q_{in}]^\top$, to this end we avail of Theorem 2. Table 1 shows the parameters considered for each ESC implemented in this work.

Figure 1 shows the input flowrate time evolution, in red the flowrate computed by the ESC and in blue the flowrate computed by the super-twisting-based ESC. Due to the dithering signal, the flowrate generated by the ESC (5) has a sinusoidal form. Please notice that both strategies present oscillations around the optimum input flowrate. In order to alleviate this phenomenon in the super-twisting-based ESC (8)-(12) we considered smaller gains of the optimization algorithm (8). Such result is depicted in the cyan curve of Figure 1. Although the

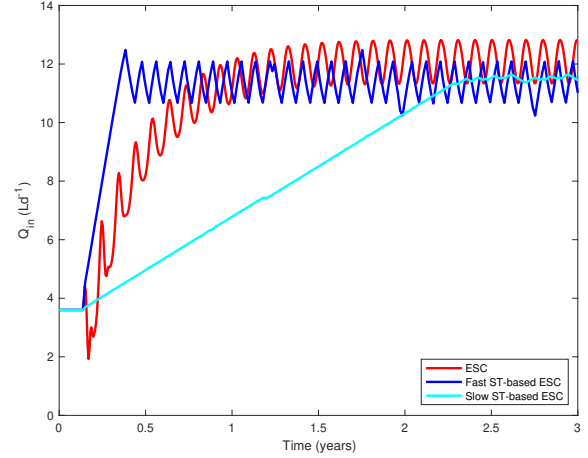


Fig. 1. Flowrate at the input of the microalgae production process.

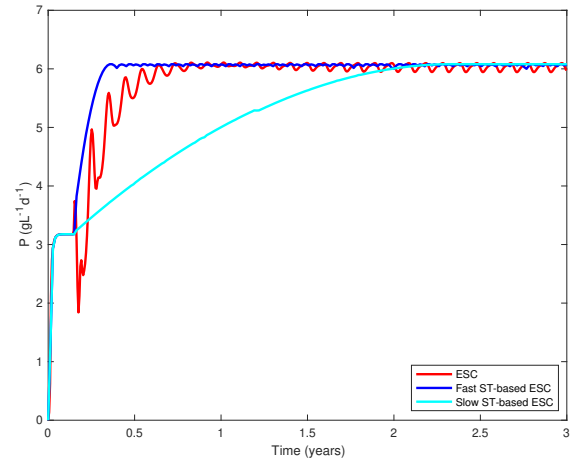


Fig. 2. Productivity of the microalgae production process.

magnitude of the oscillations are sensibly reduced, the convergence time increases. This suggests that there is a subtle tradeoff between the amplitude of the oscillations and the convergence time. It must be pointed out that oscillations of the classical ESC can be diminished by reducing both parameters, k_I and A . However, the time convergence increases considerably, in this example up to 18 years (data not shown).

In turn, Figure 2 shows the productivity time evolution, in red the productivity computed by the ESC and in blue the productivity computed by the super-twisting-based ESC. As can be observed, the ESC achieves the maximum productivity almost one year after the process beginning. On the other hand, the super-twisting-based ESC reaches the maximum productivity in less than half a year after the process beginning. Likewise, the cyan curve obtained with smaller gains of the optimization algorithm shows a larger convergence time.

Figure 3 shows the gradient estimation time evolution, in red the gradient estimated by the ESC and in blue and cyan the gradient estimated by the super-twisting-based ESC. Please notice that the key difference between the

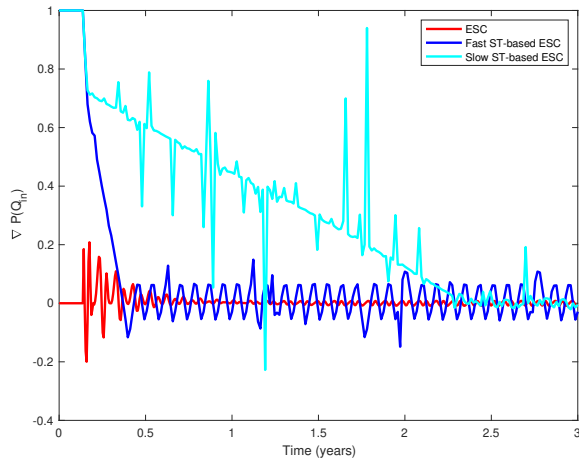


Fig. 3. Gradient of the productivity with respect to the flow rate.

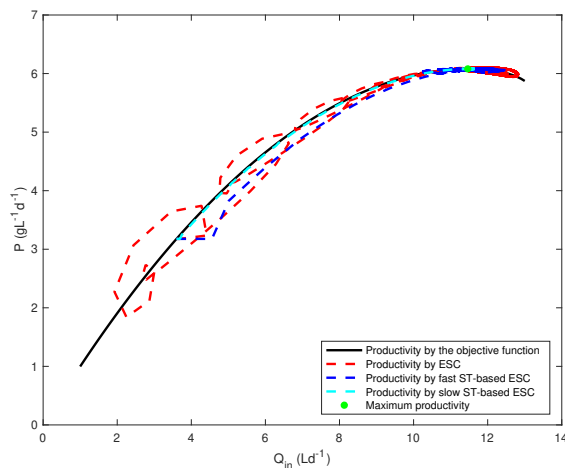


Fig. 4. Productivity vs flow rate.

ESC and the super-twisting-based ESC is that the latter one is an actual estimation of the gradient; whereas the ESC makes use of a persistent excitation signal in order to aim toward the extremum.

Figure 4 shows the productivity versus the input flowrate, in black the productivity computed by the objective function (20), in red the productivity computed by the ESC, in blue and cyan the productivity computed by the super-twisting-based ESC, and in green the point corresponding to the maximum productivity. Here we may observe that the cyan line shows the best tracking performance of the *unknown* objective function.

5. CONCLUSIONS

Here we propose an extremum seeking strategy analogous to the classical extremum seeking, in the sense that both require the same information to steer the output of a dynamical system to the maximum of an unknown input-output map in steady-state. Our algorithm consists of a super-twisting based gradient estimator that provides this information to a super-twisting based gradient-based optimizer. Furthermore, we provide a rigorous mathematical

proof of the convergence of both the optimizer and the gradient estimator. It is noteworthy that the information provided by the gradient estimator, may be used for monitoring and fault detection purposes.

A simulation example showed the feasibility of our scheme in a microalgae production photobioreactor. In this example we outperform the ESC results, since we are able to converge quicker (with similar oscillation amplitudes) or with smaller oscillation amplitudes (but larger convergence time). In addition, please notice that the optimization period used by the ESC (two days) is shorter than the optimization period used by the super-twisting-based ESC (five days). Hence, even the slow super-twisting-based ESC needs less iterations to converge to the maximum productivity than the ESC (146 iterations of the slow super-twisting-based ESC vs. 273 of the ESC).

REFERENCES

- Angulo, M. (2015). Nonlinear extremum seeking inspired on second order sliding modes. *Automatica*, 57, 51–55.
- Ariyur, K. and Krstic, M. (2003). *Real-time optimization by extremum-seeking control*. Wiley-Interscience.
- Benavides, M., Coutinho, D., Hantson, A.L., Impe, J.V., and Vande Wouwer, A. (2015). Robust luenberger observers for microalgal cultures. *Journal of Process Control*, 36, 55–63.
- Dewasme, L., Feudjio Letchindjio, C., Torres, I., and Vande Wouwer, A. (2017). Micro-algae productivity optimization using extremum-seeking control. In *Proceedings of the 25th Mediterranean Conference on Control and Automation*, 672–677.
- Lara-Cisneros, G., Aguilar-Lopez, R., and Femat, R. (2015). On the dynamic optimization of methane production in anaerobic digestion via extremum-seeking control approach. *Computers and Chemical Engineering*, 75, 49–59.
- López-Caamal, F. and Moreno, J.A. (2019). Generalised multivariable supertwisting algorithm. *International Journal of Robust and Nonlinear Control*, 29(3), 634–660.
- Nocedal, J. and Wright, S. (2000). *Numerical optimization*. Springer, 2nd. edition edition.
- Shtessel, Y., Edwards, C., Fridman, L., and Levant, A. (2014). *Sliding mode control and observation*. Springer.
- Solis, C., Clempner, J., and Poznyak, A. (2019). Extremum seeking by a dynamic plant using mixed integral sliding mode controller with synchronous detection gradient estimation. *International Journal of Robust and Nonlinear Control*, 29(3), 702–714.
- Tan, Y., Li, Y., and Mareels, I. (2013). Extremum seeking for constrained inputs. *IEEE Transactions on Automatic Control*, 58(9), 2405–2410.
- Vargas, A., Moreno, J., and Vande Wouwer, A. (2015). Super-twisting estimation of a virtual output for extremum-seeking output feedback control of bioreactors. *Journal of Process Control*, 35, 41–49.
- Yu, H. and Ozguner, U. (2003). Smooth extremum-seeking control via second order sliding mode. In *Proceedings of the American Control Conference*, 3248–3256.
- Zeng, T., Ren, X., Li, G., and Zhang, Y. (2018). Sliding mode extremum seeking control of motor driving nonlinear system. In *Proceedings of the 37th Chinese Control Conference*, 2759–2764.
- Zhang, C. and Ordóñez, R. (2012). *Extremum-seeking control and applications: a numerical optimization-based approach*. Springer.